Electronic Supplementary Material (ESI) for Dalton Transactions.

Supplementary Material for

NO_x^- Anion Recognition by Bimetallic Cryptates: Selectivity for Nitrite over Nitrate

Taraknath Chattopadhyay,[†a] Anju B. S.,[†a] Shourya Gupta, [†a] Ananya S.,[a] Jeffery A. Bertke,[b] Subrata Kundu*[a]

[a]School of Chemistry, Indian Institute of Science Education and Research, Thiruvananthapuram 695551, India

[b]Department of Chemistry, Georgetown University, Box 571227, Washington, D. C. 20057-1227, United States

[†]Equal contributions of these authors

*Corresponding author email: skundu@iisertvm.ac.in

Table of Contents **S1**

1. General Instrumentation and Physical Methods.

The preparation and handling of air-sensitive chemicals were performed under dry argon/ nitrogen atmosphere by utilizing standard Schlenk techniques. ^{1}H and ^{13}C NMR spectra were recorded on a Bruker Advance III 500 MHz NMR spectrometer at room temperature unless otherwise noted. The chemical shift (δ) values are expressed in ppm relative to tetramethylsilane, whereas the residual ^{1}H, ^{13}C signals of the deuterated solvent served as an internal standard. Elemental analyses were performed on an Elementar Vario Micro Cube CHNS analyzer. UV-vis spectra were recorded on an Agilent 8454 Diode Array spectrometer equipped with stirrer and Unisoku USP-203 cryostats for variable temperature (-105 °C to 90 °C) experiments. Solutions for UV-vis analysis were prepared freshly by dissolving analytically pure compounds in anhydrous solvents. The molar extinction coefficients of different isolated complexes were determined from the Beer's law plot (absorbance *vs* concentration) with at least four different concentrations. IR spectra (with spectral resolution of 4 cm^{-1}) were collected on a Shimadzu IRPrestige-21 FTIR spectrometer by using KBr pellet method. The intensities of the vibrational bands are abbreviated as follows: s = strong, m = medium, w = weak, vw = very weak, and br = broad. Powder X-ray diffraction data were collected employing an X'pert PRO (PANalytics) powder diffractometer equipped with a Cu K_α (λ = 1.5405 Å) radiation source. Details of single crystal X-ray crystallography and DFT calculations appear in Sections 9 and 10, respectively.

2. Materials.

All chemicals were purchased from standard vendors (e.g. Sigma-Aldrich, Spectrochem, Strem Chemicals, TCI) and used without further purification unless otherwise mentioned. Molecular sieves (4A, 4-8 mesh beads) were activated in *vacuo* at 220 °C for 24 h. Anhydrous solvents were sparged with nitrogen and stored over activated molecular sieves under nitrogen atmosphere.

Azacryptand **pC**,[S1] $[pCZn_2](ClO_4)_4$,[S2] $[pCCu_2](ClO_4)_4$[S3] were synthesized and characterized according to the literature procedures.

Caution! While we did not encounter any problem, metal perchlorate complexes with organic ligands are potentially explosive. They should be prepared and handled with care and only in small quantities at a time.

3. Synthesis and Characterization of [pCZn$_2$(μ-ONO)](ClO$_4$)$_3$ (1a).

Method A. To a solution of zinc(II) perchlorate hexahydrate $Zn(ClO_4)_2 \cdot 6H_2O$ (0.306 g, 0.822 mmol) in anhydrous methanol (~5 mL), $NaNO_2$ (0.028 g, 0.411 mmol) was added and stirred for ½ h at room temperature. To the resultant mixture, a solution of azacryptand pC (0.250 g, 0.411 mmol) in methanol (~3 mL) was added dropwise and the reaction mixture was stirred at room temperature. After stirring for 12 h, the reaction mixture was filtered to isolate the colorless residue. The residue was washed with methanol and diethyl ether, then it was dried under vacuum to obtain a colorless powder (0.385 g, 0.358 mmol) in 87% yield.

Method B. To a solution of zinc(II) perchlorate hexahydrate $Zn(ClO_4)_2 \cdot 6H_2O$ (0.306 g, 0.822 mmol) in anhydrous methanol (~6 mL), a solution of azacryptand pC (0.250 g, 0.411 mmol) in methanol (~3 mL) was added dropwise and the reaction mixture was stirred at room temperature for ½ h. To the resultant suspension, $NaNO_2$ (0.028 g, 0.411 mmol) was added. After stirring for 12 h, the reaction mixture was filtered to isolate a colorless residue, which was washed with methanol, diethyl ether and dried under vacuum to yield a colorless powder of **1a** (0.428 g, 0.398 mmol) in 97% yield.

Crystals suitable for single crystal X-ray crystallography were grown from vapor diffusion of diethyl ether to a solution of complex **1a** in dimethylformamide. Anal. Calcd for [pCZn$_2$(μ-ONO)](ClO$_4$)$_3$ (**1a**) $C_{36}H_{54}N_9O_{14}Cl_3Zn_2$: C, 40.26; H, 5.07; N, 11.74. Found: C, 40.44; H, 5.03; N, 11.47. FTIR (KBr pellet): 3431 (s, br), 3284 (m), 3122 (w), 2951-2926 (w), 2875 (m), 2374 (w), 2017 (w), 1620 (w), 1517 (w), 1467 (m), 1444 (s), 1361 (w), 1215 (m, NO_2^-), 1143 (s, ClO_4^-), 1095 (s, ClO_4^-), 1020 (s), 999 (w), 937 (m), 883 (m), 806 (s), 746 (w), 628 (s), 567 (s) (Figure S1). Purity of the bulk material was additionally confirmed by powder XRD (Figure S2).

4. Synthesis and Characterization of [pCCu$_2$(μ-ONO)](ClO$_4$)$_3$ (2a).

Method A. [pCCu$_2$(μ-ONO)](ClO$_4$)$_3$ (**2a**) was obtained as green powder by following the same procedures as described for [pCZn$_2$(μ-ONO)](ClO$_4$)$_3$ (**1a**) in Section 3. To a blue colored solution of copper(II) perchlorate hexahydrate $Cu(ClO_4)_2 \cdot 6H_2O$ (1.218 g, 3.289 mmol) in anhydrous methanol (~15 mL), $NaNO_2$ (0.113 g, 1.645 mmol) was added and the resulting green solution was stirred for ½ h at room temperature. To this, a solution of azacryptand pC (1.000 g, 1.645 mmol) in methanol (~5 mL) was added dropwise and the reaction mixture was stirred at room temperature to obtain a green precipitate. After stirring for 12 h, the reaction mixture was filtered to isolate the green residue. The residue was washed with methanol and diethyl ether, then it was dried under vacuum to obtain a green powder (1.700 g, 1.588 mmol) in 95% yield.

Method B. To a solution of copper(II) perchlorate hexahydrate $Cu(ClO_4)_2 \cdot 6H_2O$ (0.305 g, 0.822 mmol) in anhydrous methanol (~6 mL), a solution of azacryptand pC (0.250 g, 0.411 mmol) in methanol (~3 mL) was added dropwise and the reaction mixture was stirred at room temperature for ½ h. To the resultant suspension, $NaNO_2$ (0.028 g, 0.411 mmol) was added and the color of the solution rapidly turned green. After stirring for 12 h, the reaction mixture was filtered to isolate the green residue, which was washed with methanol, diethyl ether and dried under vacuum to yield a green powder (0.332 g, 0.310 mmol) in 76% yield.

Crystals suitable for single crystal X-ray crystallography were grown from vapor diffusion of diethyl ether to a solution of the complex in dimethylformamide. Anal. Calcd for [pCCu$_2$(μ-ONO)](ClO$_4$)$_3$ (**2a**), $C_{36}H_{54}N_9O_{14}Cl_3Cu_2$: C, 40.40; H, 5.09; N, 11.78. Found: C, 40.87; H, 5.20; N, 11.77. UV-Vis (Acetonitrile, 25 °C): λ_{max}/nm (ε/M^{-1}cm^{-1}) = 675 (180), 855 (430) (Figure S3). FTIR (KBr pellet): 3439 (s), 3298 (w), 2926-2881 (w), 1637 (m), 1469 (w), 1444 (m), 1381 (w), 1273 (w), 1211 (vw), 1181 (w), 1143 (m), 1116 (s, ClO_4^-), 1089 (s, ClO_4^-), 1006 (w), 925 (w), 810 (m), 626 (m) (Figure S4). Purity of the bulk material was additionally confirmed by powder XRD (Figure S5). Room temperature (298 K) solution magnetic moment of **2a** was determined using Evans method. 13.8 mM solution of complex **2a** in d_6-DMSO was prepared by dissolving microcrystalline complex **2a** in d_6-DMSO and mesitylene was used as standard. The Evans Method calculation provides $\mu_{eff} \approx 2.39$ μB.

5. Synthesis and Characterization of [pCZn$_2$(μ-ONO$_2$)](ClO$_4$)$_3$ (1b).

To a solution of zinc(II) perchlorate hexahydrate Zn(ClO$_4$)$_2$·6H$_2$O (0.306 g, 0.822 mmol) in anhydrous methanol (~5 mL), NaNO$_3$ (0.035 g, 0.411 mmol) was added and stirred for ½ h at room temperature. To the resultant reaction mixture, a solution of azacryptand pC (0.250 g, 0.411 mmol) in methanol (~3 mL) was added dropwise and stirred at room temperature to obtain a colorless precipitate. After stirring for 12 h, the reaction mixture was filtered to isolate the colorless residue, which was washed with methanol and diethyl ether, then it was dried under vacuum to obtain a colorless powder (0.418 g, 0.383 mmol) in 93% yield. Several attempts to obtain crystals suitable for single crystal X-ray diffraction were unsuccessful. Anal. Calcd for [pCZn$_2$(μ-ONO$_2$)](ClO$_4$)$_3$ (**1b**), $C_{36}H_{54}N_9O_{15}Cl_3Zn_2$: C, 39.67; H, 4.99; N, 11.57. Found: C, 39.90; H, 5.26; N, 11.32. FTIR (KBr pellet): 3431 (s, br), 3294 (w), 3250 (w), 2872 (m), 1627 (m), 1469 (w), 1444 (m), 1382 (s, NO_3^-), 1336 (w), 1093 (s, ClO_4^-), 1022 (w), 933 (w), 887 (m), 806 (s), 750 (w), 628 (s), 501 (w). (Figure S6).

6. Synthesis and Characterization of [pCCu$_2$(μ-ONO$_2$)](ClO$_4$)$_3$ (2b).

To a blue colored solution of copper(II) perchlorate hexahydrate Cu(ClO$_4$)$_2$·6H$_2$O (0.122 g, 0.328 mmol) in anhydrous methanol (~3 mL), NaNO$_3$ (0.014 g, 0.164 mmol) was added and stirred for ½ h at room temperature. To the resultant reaction mixture, a solution of azacryptand pC (0.100 g, 0.164 mmol) in methanol (~1 mL) was added dropwise and it was stirred at room temperature to obtain a blue precipitate. After stirring for 12 h, the reaction mixture was filtered to isolate the blue residue, which was washed with methanol and diethyl ether, then it was dried under vacuum to obtain a blue powder **2b** (0.162 g, 0.149 mmol) in 91% yield. Several attempts to obtain crystals suitable for single crystal X-ray diffraction were unsuccessful. Anal. Calcd for [pCCu$_2$(μ-ONO$_2$)](ClO$_4$)$_3$ (**2b**), $C_{36}H_{54}N_9O_{15}Cl_3Cu_2 \cdot H_2O$: C, 39.15; H, 5.14; N, 11.41. Found: C, 38.91; H, 5.02; N, 11.27. UV-Vis (Acetonitrile, 25 °C): λ_{max}/nm (ε/M^{-1}cm^{-1}) = 680 (400), 820 (560) (Figure S8). FTIR (KBr pellet): 3423 (s, br), 3248 (w), 3167 (w), 2877 (w), 1624 (w), 1571 (w), 1446 (m), 1382 (s, NO_3^-), 1305 (w), 1209 (w), 1145 (s), 1112 (s, ClO_4^-), 1089 (s, ClO_4^-), 1014 (w), 927-848 (w), 808 (m), 754 (w), 603 (s), 599 (w) (Figure S10). Room temperature (298 K) solution magnetic moment of **2b** was determined using Evans method. 13.8 mM solution of complex **2b** in *d*$_6$-DMSO was prepared by dissolving microcrystalline complex **2b** in *d*$_6$-DMSO and mesitylene was used as standard. The Evans method calculation provides $\mu_{eff} \approx 2.37$ μB.

7. NO_2^- *versus* NO_3^- Recognition Selectivity for $[pCZn_2]^{4+}$

i) Substitution of NO_3^- by NO_2^- from $[pCZn_2(\mu\text{-}ONO_2)](ClO_4)_3$ (1b)

To a suspension of $[pCZn_2(\mu\text{-}ONO_2)](ClO_4)_3$ (**1b**) (0.100 g, 0.092 mmol) in anhydrous methanol (~8 mL) and a few drops of dimethylacetamide, a solution of $NaNO_2$ (0.006 g, 0.092 mmol) in methanol (~1 mL) was added. The reaction mixture was stirred for 12 h and then filtered to isolate a colorless residue. The residue was washed with methanol and diethyl ether, then dried under vacuum to obtain a colorless powder (0.068 g, 0.063 mmol) in 69% yield. The characterization of the powder was done using FTIR spectroscopy (Figure S12) and powder X-Ray diffraction techniques (Figure S13, blue trace). Comparison of FTIR spectrum and powder XRD pattern with those of the authentic complex $[pCZn_2(\mu\text{-}ONO)](ClO_4)_3$ (**1a**) show the formation of $[pCZn_2(\mu\text{-}ONO)](ClO_4)_3$ (**1a**). Anal. Calcd for the desired product $[pCZn_2(\mu\text{-}ONO)](ClO_4)_3$ (**1a**) $C_{36}H_{54}N_9O_{14}Cl_3Zn_2$: C, 40.26; H, 5.07; N, 11.74. Found: C, 40.06; H, 5.04; N, 11.83. FTIR (KBr pellet): 3439 (s, br), 3286 (m), 2951-2873 (w), 1639-1516 (w), 1448 (m), 1382 (w), 1365 (w), 1271 (m), 1215 (m, NO_2^-), 1143 (s), 1112 (s, ClO_4^-), 1091 (s, ClO_4^-), 1020 (m), 999 (w), 937 (w), 885 (w), 808 (m), 746 (w), 628 (s), 569 (m) (Figure S12, blue trace).

ii) Competition between NO_2^- and NO_3^- for the cavity of $[pCZn_2]^{4+}$

To a solution of zinc(II) perchlorate hexahydrate $Zn(ClO_4)_2{\cdot}6H_2O$ (0.123 g, 0.328 mmol) in anhydrous methanol (~5 mL), a solution of azacryptand pC (0.100 g, 0.164 mmol) in methanol (~5 mL) was added dropwise and the reaction mixture was stirred at room temperature for ½ h. A white precipitate formed, to which a combined solution of $NaNO_2$ (0.011 g, 0.164 mmol) and excess $NaNO_3$ (0.139 g, 1.635 mmol) in methanol (~5 mL) was added and the reaction mixture was stirred for 12 h. The residue was isolated by filtration, washed with methanol and diethyl ether, then it was dried under vacuum to obtain a colorless powder (0.166 g, 0.154 mmol) in 94% yield. Comparison of FTIR spectrum and powder XRD pattern with those of the authentic complex $[pCZn_2(\mu\text{-}ONO)](ClO_4)_3$ (**1a**) show the formation of $[pCZn_2(\mu\text{-}ONO)]^{3+}$ (**1a**) even in the presence of excess NO_3^- (Figures S12 and S13, orange trace). Anal. Calcd for desired product $[pCZn_2(\mu\text{-}ONO)](ClO_4)_3$ (**1a**) $C_{36}H_{54}N_9O_{14}Cl_3Zn_2$: C, 40.26; H, 5.07; N, 11.74. Found: C, 40.63; H, 4.92; N, 12.49. A slightly higher value of nitrogen may appear due to presence of some nitrate as impurity/ counter-anion. FTIR (KBr pellet): 3442 (s, br), 3284 (m), 2951-2873 (w), 1616 (w), 1446 (m), 1382 (s), 1350 (m), 1280 (w), 1215 (m, NO_2^-), 1143 (m), 1095 (s, ClO_4^-), 1020 (m), 997 (w), 937 (m), 883 (w), 806 (s), 746 (w), 628 (s), 565 (m) (Figure S12, orange trace).

8. NO_2^- *versus* NO_3^- Recognition Selectivity for $[pCCu_2]^{4+}$

i) Substitution of NO_3^- by NO_2^- from $[pCCu_2(\mu\text{-}ONO_2)](ClO_4)_3$ (2b)

To a blue solution of copper(II) perchlorate hexahydrate $Cu(ClO_4)_2 \cdot 6H_2O$ (0.122 g, 0.328 mmol) in anhydrous methanol (~4 mL), a solution of azacryptand pC (0.100 g, 0.164 mmol) in methanol (~1 mL) was added dropwise and the reaction mixture was stirred at room temperature for ½ h to obtain a blue precipitate. To the resultant suspension, $NaNO_3$ (0.014 g, 0.164 mmol) in anhydrous methanol (~1 mL) was added and stirred at room temperature for 3 h. To this, a solution of $NaNO_2$ (0.011 g, 0.164 mmol) in anhydrous methanol (~1 mL) was added and the color of the precipitate immediately changed to green. After stirring for 12 h, the reaction mixture was filtered to isolate the green residue, which was washed with methanol, diethyl ether and dried under vacuum to yield a green powder (0.161 g, 0.150 mmol) in 92% yield. As the nitrite vibration band in FTIR is very weak in intensity, characterization of the product was done using CHN analysis and powder X-Ray diffraction techniques (Figure S15). Anal. Calcd for desired product $[pCCu_2(\mu\text{-}ONO)](ClO_4)_3$ (**2a**) $C_{36}H_{54}N_9O_{14}Cl_3Cu_2 \cdot H_2O$: C, 39.73; H, 5.19; N, 11.68. Found: C, 39.76; H, 4.97; N, 11.69.

The reaction was also followed using UV-vis spectroscopy (Figure 4). A stock solution of $[pCCu_2](ClO_4)_4$ with 1.0 mM concentration in acetonitrile was used. A solution of $[pCCu_2](ClO_4)_4$ (2.0 mL, 1.0 mM, 2.0 μmol) in acetonitrile was taken in a quartz cuvette capped with a rubber septum. The sealed cuvette was then placed in a cryostat (at 25 °C) connected to a UV-vis spectrometer. The time-dependent UV-vis absorption spectra were collected for following the substitution reaction, after injecting a methanolic solution of $NaNO_3$ (200 μL, 20.0 mM, 4.0 μmol), followed by addition of a methanolic solution of $NaNO_2$ (200 μL, 20.0 mM, 4.0 μmol) by a syringe.

ii) Competition between NO_2^- and NO_3^- for the cavity of $[pCCu_2]^{4+}$

To a solution of copper(II) perchlorate hexahydrate $Cu(ClO_4)_2 \cdot 6H_2O$ (0.122 g, 0.328 mmol) in anhydrous methanol (~5 mL), a solution of pC (0.100 g, 0.164 mmol) in methanol (~2 mL) was added dropwise and the reaction mixture was stirred at room temperature to obtain a blue residue of $[pCCu_2](ClO_4)_4$. To the resultant suspension, a combined solution of $NaNO_2$ (0.011 g, 0.164 mmol) and excess $NaNO_3$ (0.139 g, 1.635 mmol) in methanol (~5 mL) was added. The color of the precipitate formed immediately changed to green. The residue obtained after 12 h stirring at room temperature, was isolated by filtration. It was washed with methanol and diethyl ether, then it was dried under vacuum to obtain a green powder (0.157 g, 0.146 mmol) in 90% yield. As the nitrite vibration band in FTIR is very weak in intensity, characterization of the product was done using CHN analysis and powder X-Ray diffraction techniques (Figure S15). Anal. Calcd for the desired product $[pCCu_2(\mu\text{-}ONO)](ClO_4)_3$ (**2a**) $C_{36}H_{54}N_9O_{14}Cl_3Cu_2\cdot H_2O$: C, 39.73; H, 5.19; N, 11.68. Found: C, 39.53; H, 4.99; N, 11.88.

The reaction was also followed using UV-Vis spectroscopy (Figure S14). A stock solution of $[pCCu_2](ClO_4)_4$ with 1.0 mM concentration in acetonitrile was used. A solution of $[pCCu_2](ClO_4)_4$ (2.0 mL, 1.0 mM, 2.0 μmol) in acetonitrile was taken in a quartz cuvette capped with a rubber septum. The sealed cuvette was then placed in a cryostat (at 25 °C) connected to a UV-vis spectrometer. After injecting a solution of $NaNO_2$ (4.0 μmol) and $NaNO_3$ (40.0 μmol) in methanol (200 μL) to the cuvette, time-dependent UV-vis absorption spectra were collected for following the reaction.

9. Crystallographic details.

Single crystals of each compound **1a** (CCDC 1884272) and **2a** (CCDC 1884273) were mounted under mineral oil on a glass capillary. Data for compounds **1a** and **2a** were collected at 150 K and 296 K, respectively, on a Bruker Kappa diffractometer equipped with an APEXII CCD detector and Mo fine focus sealed tube source. Both the data were collected by employing graphite monochromated Mo K_α radiation (λ = 0.7107 Å) and the data sets were processed using APEX II software. Integration of the data sets were carried out with the Bruker SAINT program. Structure solutions were performed using the SHELXTL/PC suite.[S4] Intensities were corrected for Lorentz and polarization effects and an empirical absorption correction was applied using Blessing's method as incorporated into the program SADABS.[S5] Non-hydrogen atoms were refined with anisotropic thermal parameters and hydrogen atoms were included in idealized positions.

Further comments on disorder models:

[pCZn$_2$(μ-ONO)](ClO$_4$)$_3$ (1a). The NO_2 moiety of the cation is disordered about a symmetry site and thus has been modeled using a negative PART command. Due to the symmetry of the site, the occupancy of the NO_2 group has been fixed at 1/6. The N-O distances were restrained to be 1.25 Å and the O···O distance was restrained to be 2.10 Å. The atoms were restrained to behave relatively isotropic. The ligand is disordered over two positions across a symmetry site, and was also modeled with negative PART commands. The like Zn-N, N-C, and C-C distances were restrained to be similar. Similar displacement amplitudes were imposed on disordered sites overlapping by less than the sum of van der Waals radii. The disordered atoms were restrained to behave relatively isotropic.

Both perchlorate anions are disordered. Perchlorate one is disordered over two positions, whose site occupancies refine to 77% and 23% respectively. The Cl-O distances were restrained to be similar (esd 0.01 Å). Similar displacement amplitudes were imposed on disordered sites overlapping by less than the sum of the van der Waals radii. Perchlorate two is disordered about the origin. A single oxygen atom site was modeled with a site occupancy of 2/3. By symmetry, there are six positions for this oxygen summing to a total of four oxygen atoms per chloride atom. The largest residual electron density peak is near this disordered perchlorate, however, attempts to further model the anion to account for this electron density were unsuccessful. All perchlorate atoms were restrained to behave relatively isotropic.

The model was refined as a two-component twin. The two domains are related by the twin law [-1 0 0] [0 -1 0] [0 0 1]. The ratio of the major/minor domain refines to be approximately 78/22.

$[pCCu_2(\mu\text{-}ONO)](ClO_4)_3$ (2a). The NO_2 moiety of the cation is disordered about a symmetry site and thus has been modeled using a negative PART command. Due to the symmetry of the site, the occupancy of the NO_2 group has been fixed at 1/6. The N-O distances were restrained to be 1.25 Å and the O···O distance was restrained to be 2.10 Å. The atoms were restrained to behave relatively isotropic. Both perchlorate anions are disordered. Perchlorate one is disordered over two positions, whose site occupancies refine to 58% and 42% respectively. The Cl-O distances were restrained to be similar (esd 0.01 Å). Similar displacement amplitudes were imposed on disordered sites overlapping by less than the sum of the van der Waals radii. Perchlorate two is disordered about the origin. A single oxygen atom site was modeled with a site occupancy of 2/3. By symmetry, there are six positions for this oxygen summing to a total of four oxygen atoms per chloride atom. All perchlorate atoms were restrained to behave relatively isotropic.

The amine hydrogen atom was located in the difference map. The N-H distance was restrained to be 0.89 Å.

10. Computational details

Density Functional Theory **(**DFT) calculations were carried out using the Gaussian09 program package[S6] at B3LYP/TZVP level of theory.[S7,S8] Natural population analysis (NPA) was performed from NBO calculations as described earlier.[S9] Visualization, structural and molecular orbital analyses were done using GaussView 5.0,[S10] Chimera,[S11] and CCDC-Mercury[S12] software packages.

Initial coordinates of the cationic parts $[\mathrm{pCM_2}(\mu\text{-ONO})]^{3+}$ for **1a** and **2a** were obtained from the primary orientations of the disordered part (PART 1) in the X-ray crystal structure of **1a**. As the full system consists a large number of atoms, geometry optimizations were carried out using frozen cryptand core and the coordinates of M, O, N sites were unrestricted. A similar strategy has been used previously for a closely related system.[S3] Moreover, the absence of imaginary frequencies in the frequency calculations confirmed the true minima.

11. Figures and Tables

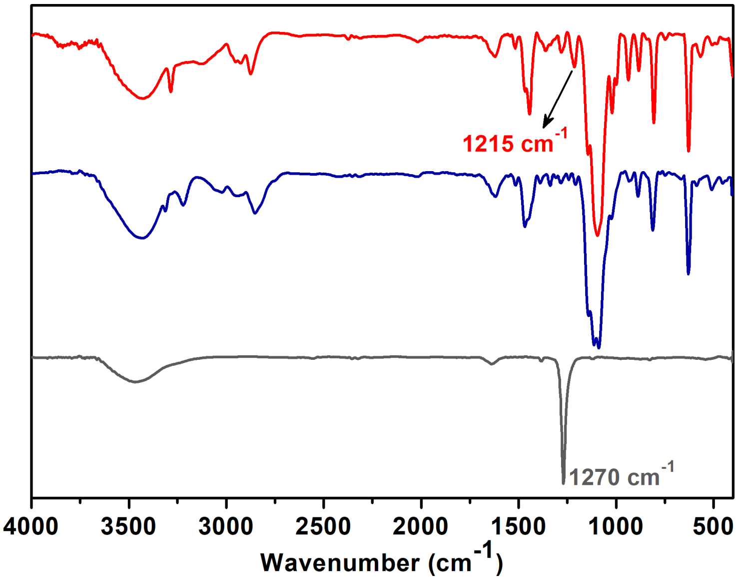

Figure S1. FTIR (KBr pellet) spectra of [pCZn$_2$(μ-ONO)](ClO$_4$)$_3$ (**1a**) (red trace), [pCZn$_2$](ClO$_4$)$_4$ (blue trace), and NaNO$_2$ (grey trace). The vibrational band for encapsulated nitrite anion in **1a** appears at 1215 cm^{-1} and free nitrite anion in NaNO$_2$ appears at 1270 cm^{-1}.

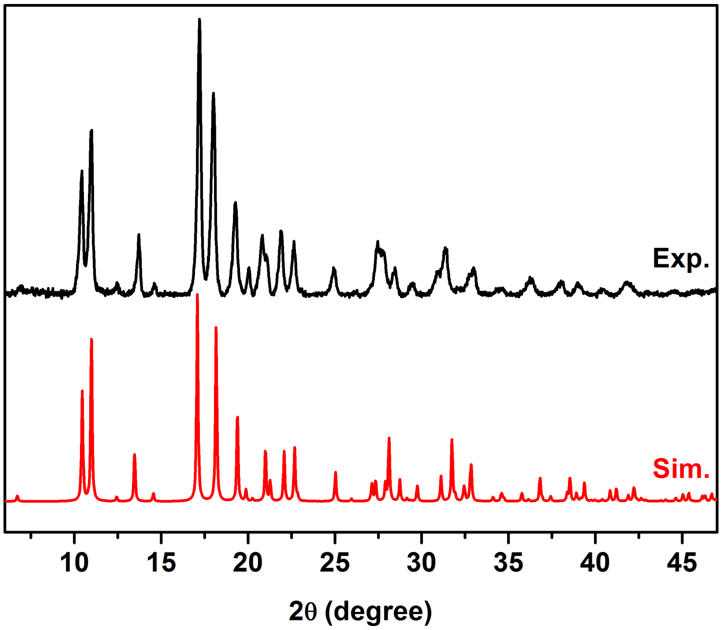

Figure S2. PXRD experimental (black trace) and simulated (red trace) patterns of [pCZn$_2$(μ-ONO)](ClO$_4$)$_3$ (**1a**).

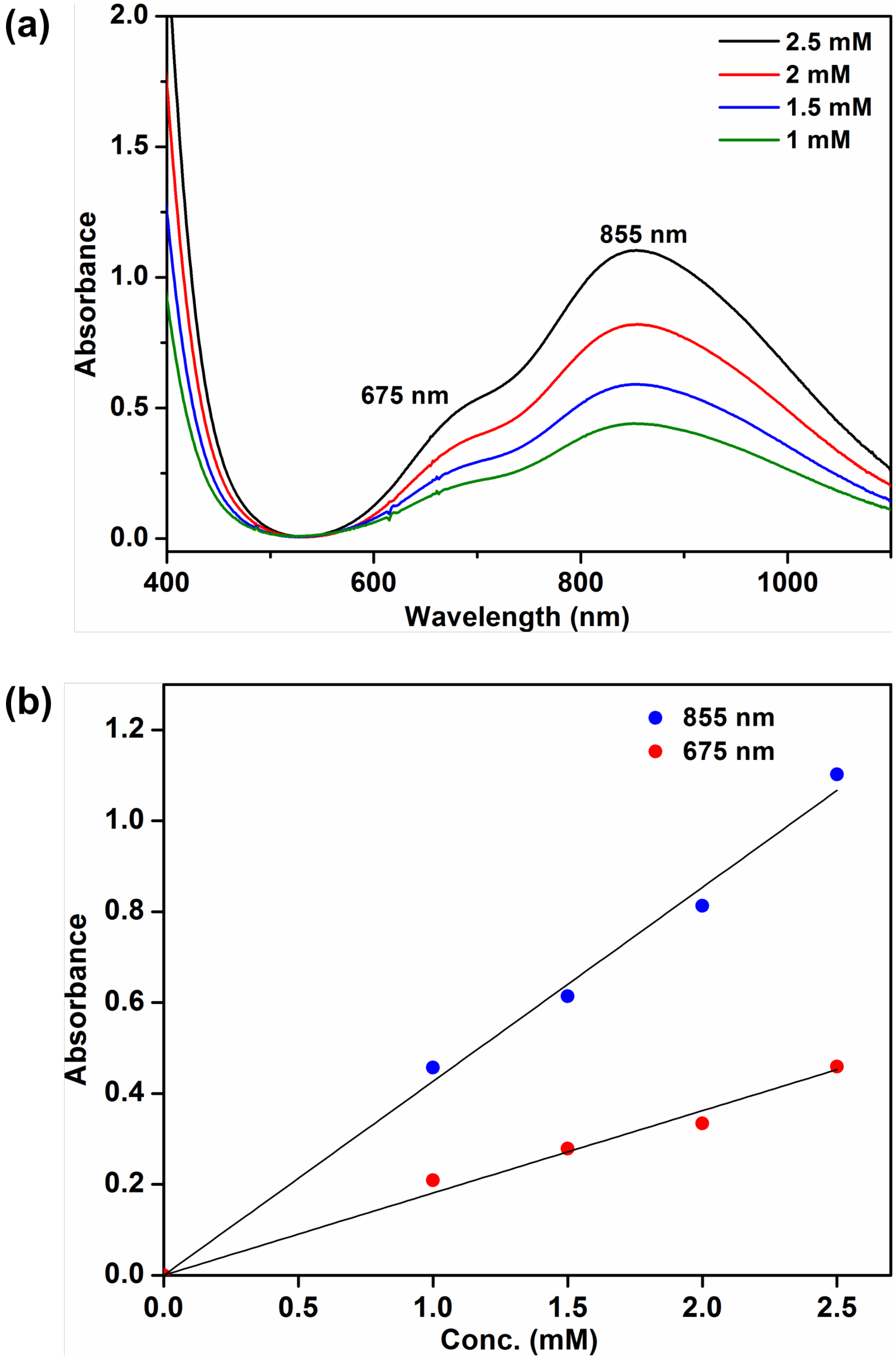

Figure S3. (a) UV-vis spectra of [pCCu$_2$(μ-ONO)](ClO$_4$)$_3$ (**2a**) in acetonitrile at 25 ºC at different concentrations. (b) Beer's law (Absorbance *versus* concentration) plot for [pCCu$_2$(μ-ONO)](ClO$_4$)$_3$ (**2a**) depicts λ_{sh} = 675 nm (ε = 180 M^{-1}cm^{-1}) and λ_{max} = 855 nm (ε = 430 M^{-1}cm^{-1}).

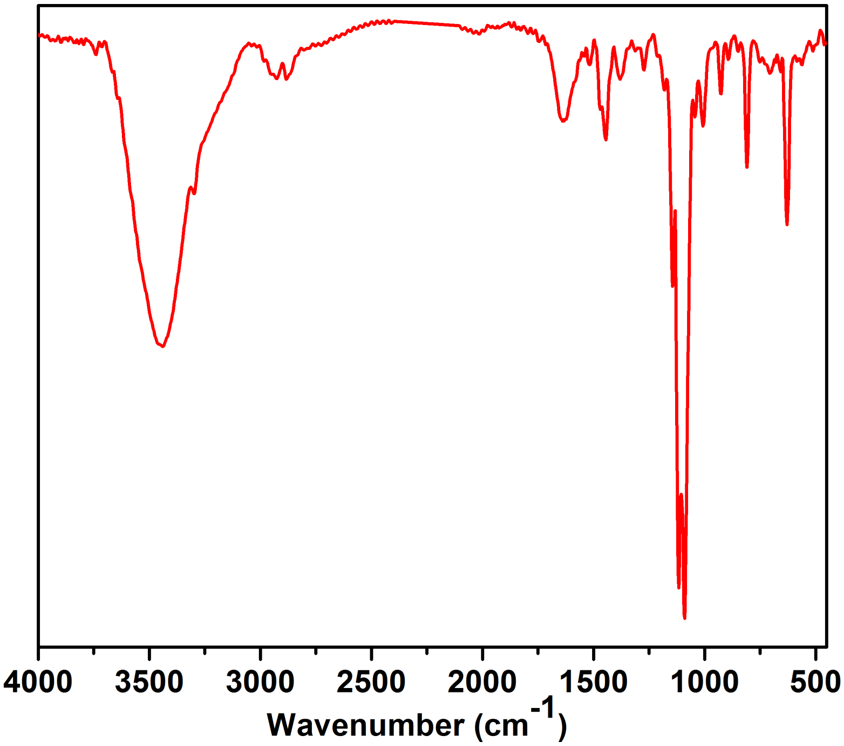

Figure S4. FTIR (KBr pellet) spectrum of [pCCu$_2$(μ-ONO)](ClO$_4$)$_3$ (**2a**).

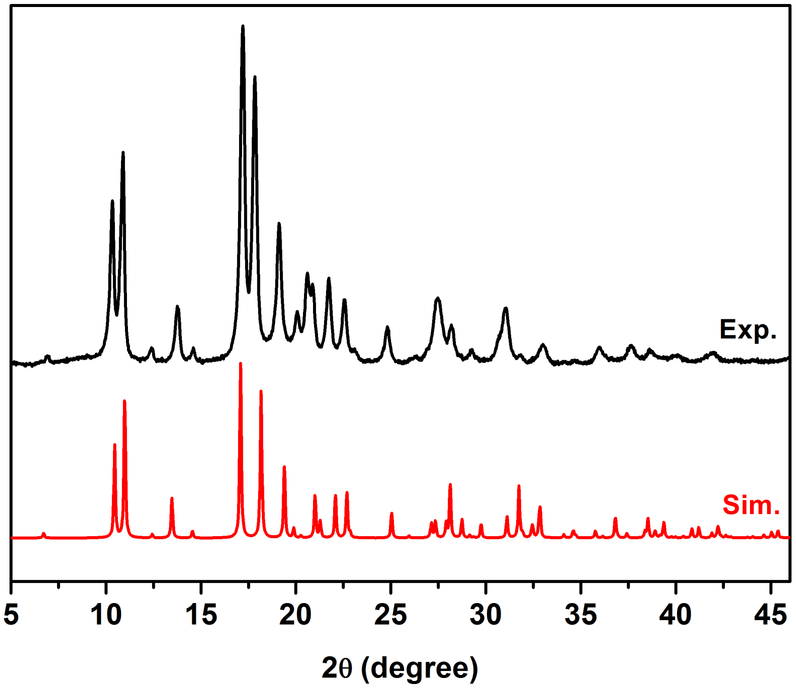

Figure S5. PXRD experimental (black trace) and simulated (red trace) patterns of [pCCu$_2$(μ-ONO)](ClO$_4$)$_3$ (**2a**).

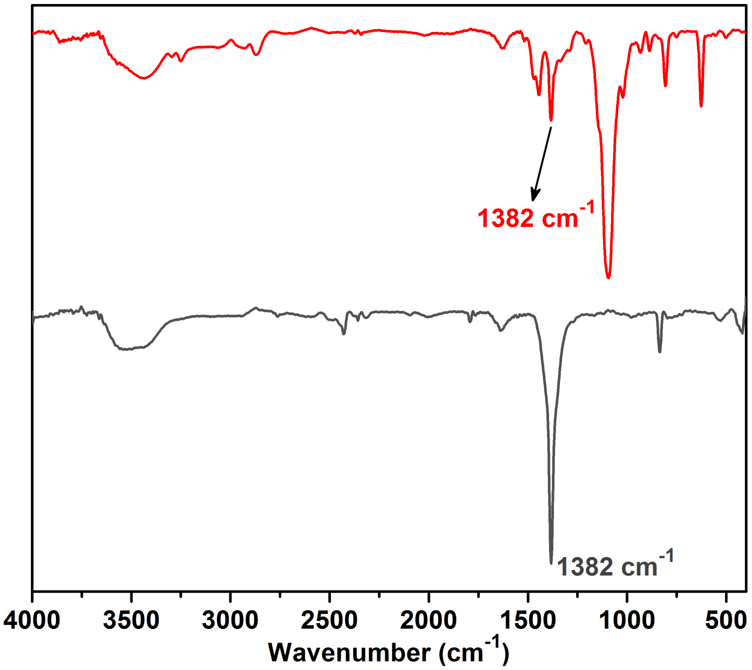

Figure S6. FTIR (KBr pellet) spectra of [pCZn$_2$(μ-ONO$_2$)](ClO$_4$)$_3$ (**1b**) (red trace) and NaNO$_3$ (grey trace). The vibrational band for nitrite anion in **1b** appears at 1382 cm^{-1} and free nitrate anion in NaNO$_3$ appears at 1382 cm^{-1}.

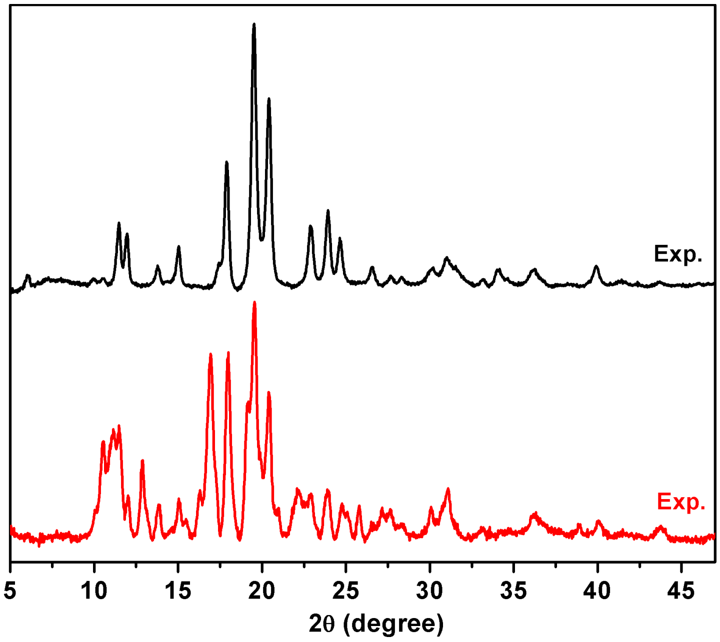

Figure S7. PXRD experimental patterns of [pCZn$_2$(μ-ONO$_2$)](ClO$_4$)$_3$ (**1b**) (red trace) and [pCZn$_2$](ClO$_4$)$_4$ (black trace).

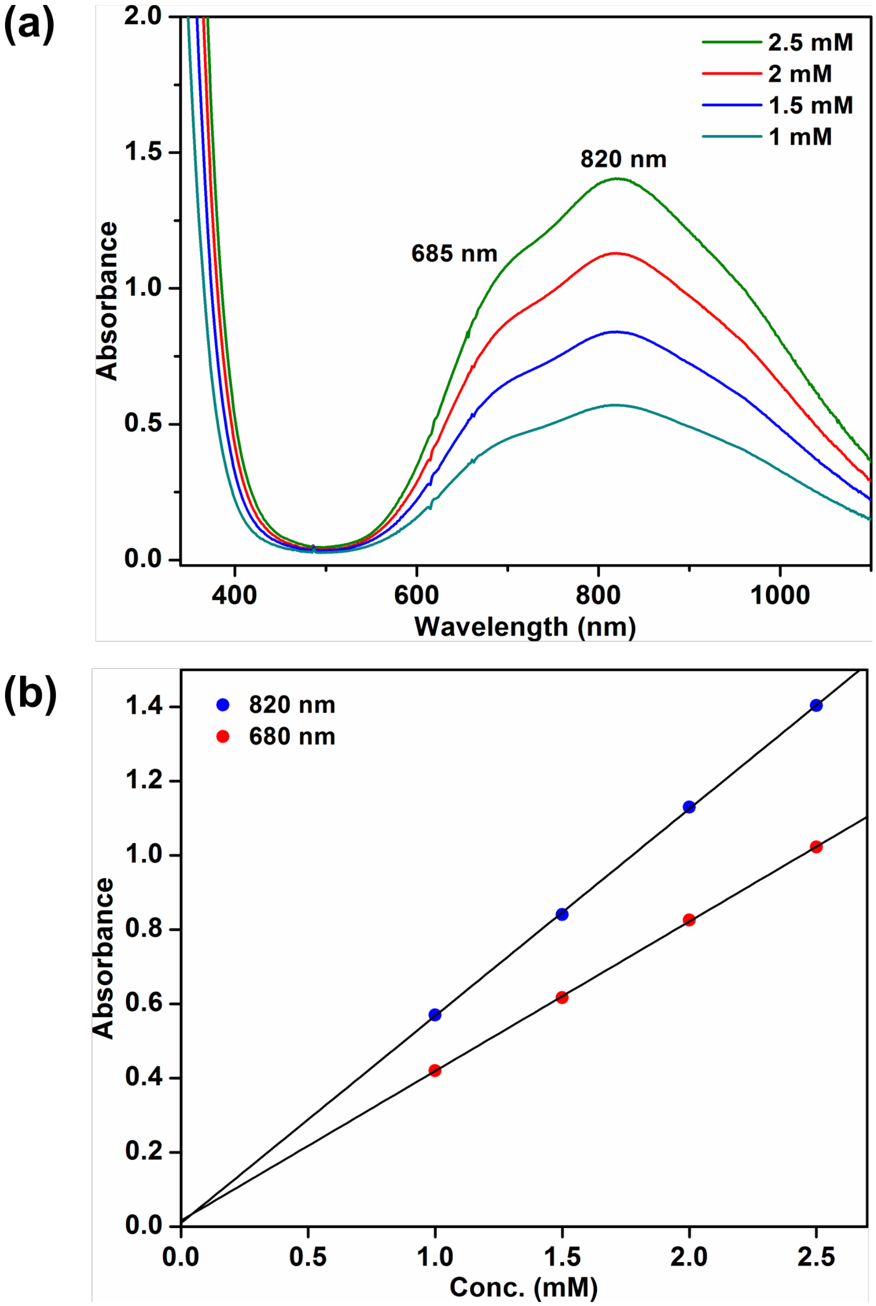

Figure S8. (a) UV-vis spectra of $[pCCu_2(\mu\text{-}ONO_2)](ClO_4)_3$ (**2b**) in acetonitrile at 25 ºC at different concentrations. (b) Beer's law (Absorbance *versus* concentration) plot for $[pCCu_2(\mu\text{-}ONO_2)](ClO_4)_3$ (**2b**) depicts λ_{max} = 820 nm (ε = 560 $M^{-1}cm^{-1}$) with λ_{sh} = 685 nm (ε = 400 $M^{-1}cm^{-1}$).

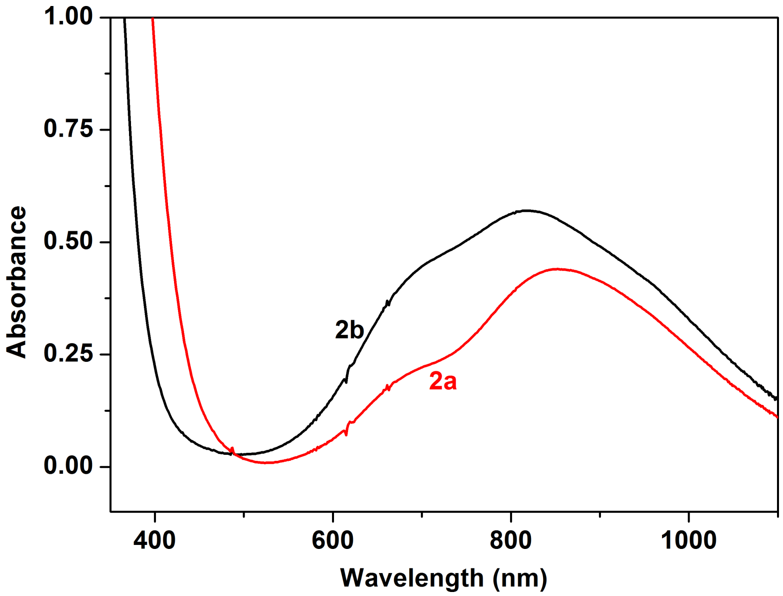

Figure S9. Comparison of UV-vis spectra of [pCCu$_2$(μ-ONO)](ClO$_4$)$_3$ (**2a**) (red trace) and [pCCu$_2$(μ-ONO$_2$)](ClO$_4$)$_3$ (**2b**) (black trace) in acetonitrile at 25 °C.

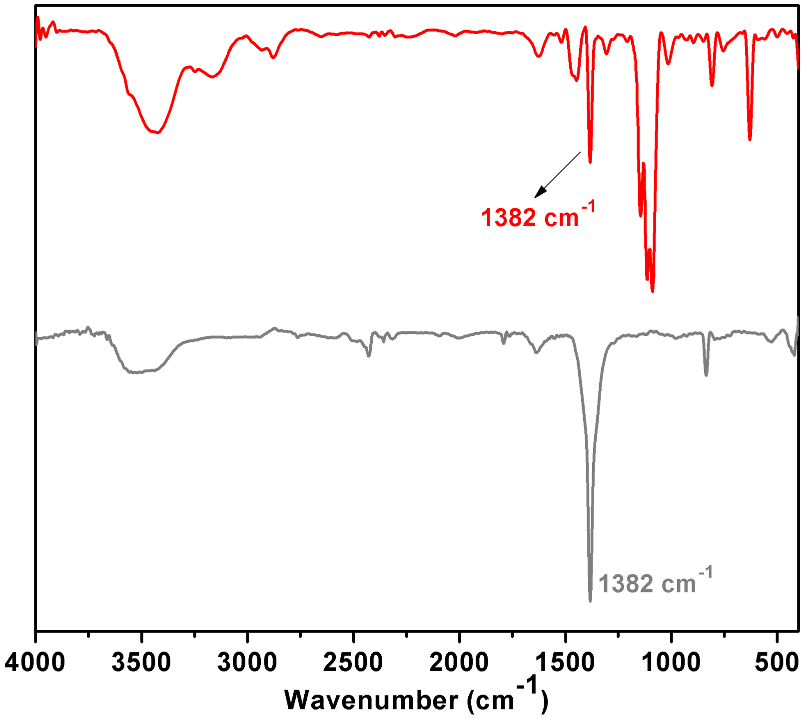

Figure S10. FTIR (KBr pellet) spectra of [pCCu$_2$(μ-ONO$_2$)](ClO$_4$)$_3$ (**2b**) (red trace) and NaNO$_3$ (grey trace). The vibrational band for nitrite anion in **2b** appears at 1382 cm^{-1} and free nitrate anion in NaNO$_3$ appears at 1382 cm^{-1}.

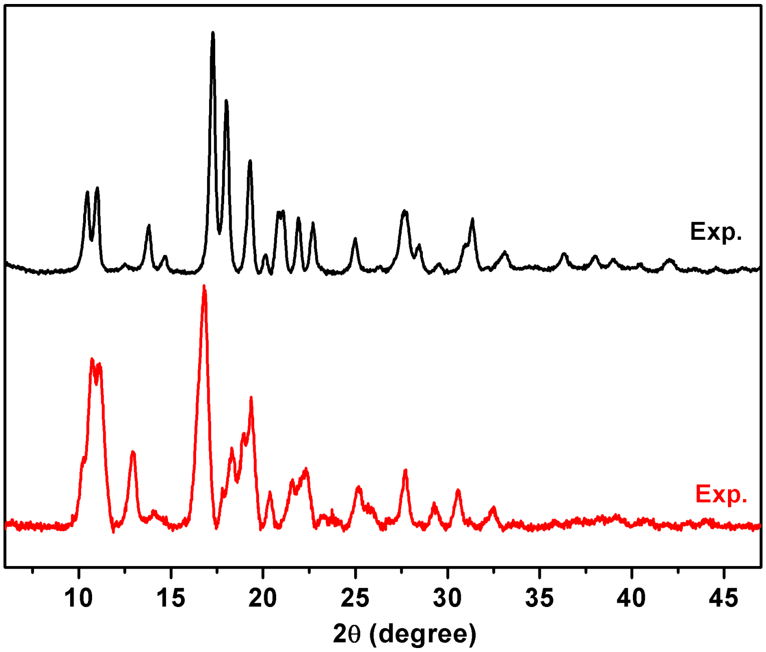

Figure S11. PXRD experimental patterns of [pCCu$_2$(μ-ONO$_2$)](ClO$_4$)$_3$ (**1b**) (red trace) and [pCCu$_2$](ClO$_4$)$_4$ (black trace).

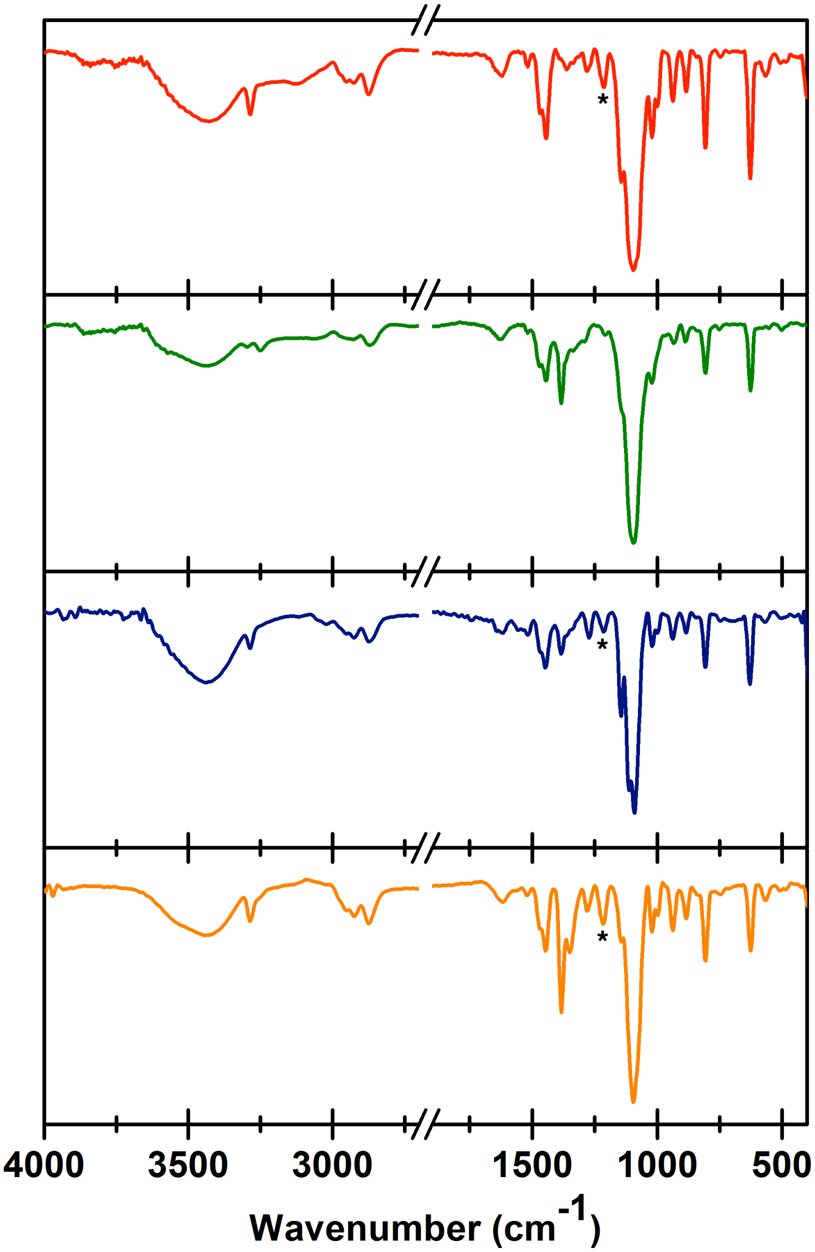

Figure S12. Comparison of FTIR (KBr pellet) spectra of [pCZn$_2$(μ-ONO)](ClO$_4$)$_3$ (**1a**) (red trace), [pCZn$_2$(μ-ONO$_2$)](ClO$_4$)$_3$ (**1b**) (green trace), [pCZn$_2$(μ-ONO)](ClO$_4$)$_3$ obtained from a reaction of **1b** + NaNO$_2$ (blue trace), and [pCZn$_2$(μ-ONO)](ClO$_4$)$_3$ obtained from a reaction of [pCZn$_2$]$^{4+}$ and a 1:10 mixture of NaNO$_2$ and NaNO$_3$ (orange trace). The vibrational band for nitrite anion in [pCZn$_2$(μ-ONO)]$^{3+}$ is marked with asterisk.

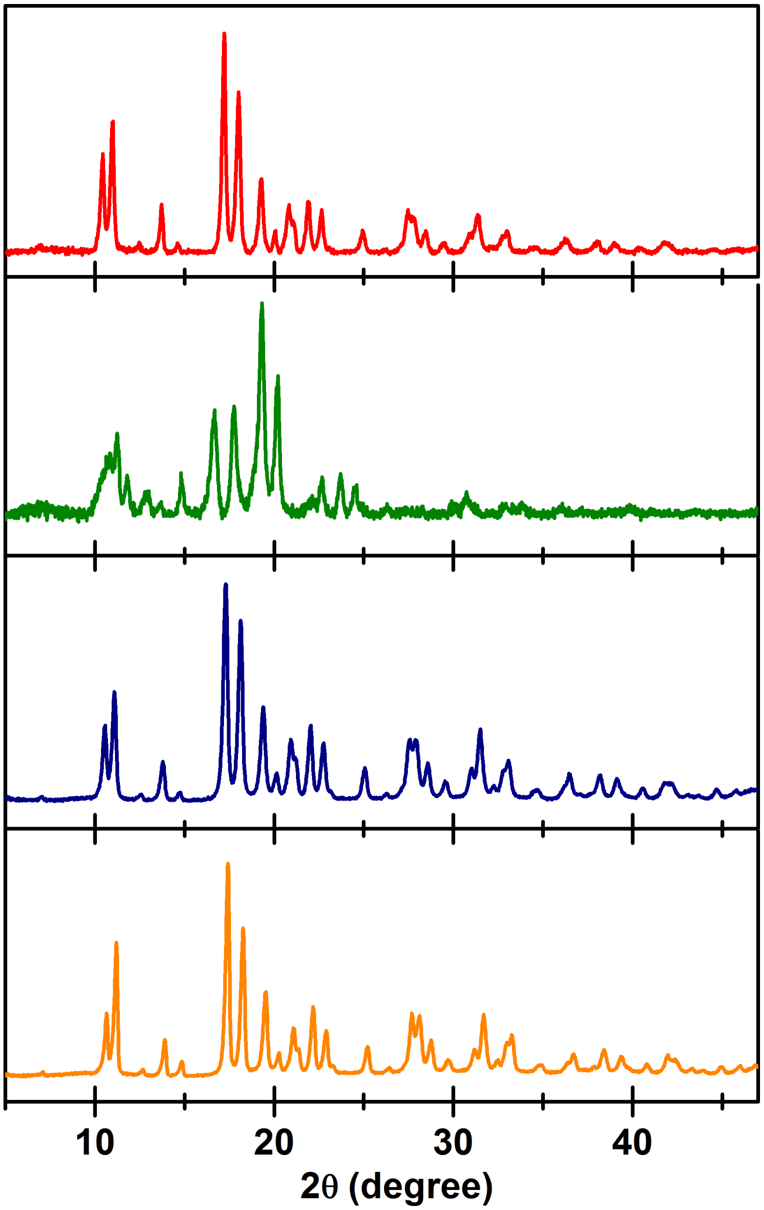

Figure S13. Comparison of PXRD patterns of [pCZn$_2$(μ-ONO)](ClO$_4$)$_3$ (**1a**) (red trace), [pCZn$_2$(μ-ONO$_2$)](ClO$_4$)$_3$ (**1b**) (green trace), [pCZn$_2$(μ-ONO)](ClO$_4$)$_3$ obtained from a reaction of **1b** + NaNO$_2$ (blue trace), and [pCZn$_2$(μ-ONO)](ClO$_4$)$_3$ obtained from a reaction of [pCZn$_2$]$^{4+}$ and a 1:10 mixture of NaNO$_2$ and NaNO$_3$ (orange trace).

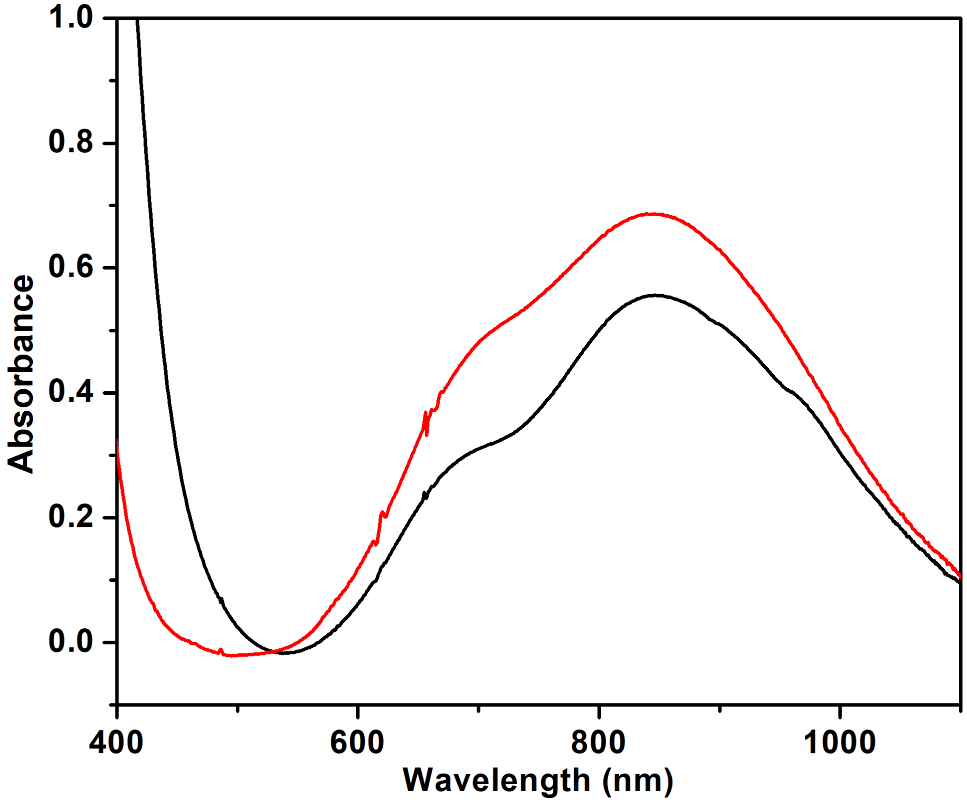

Figure S14. Changes in the UV-vis absorption features of $[pCCu_2](ClO_4)_4$ in acetonitrile (2.0 mL, 1.0 mM, 2.0 µmol) (red trace) upon addition of a methanolic solution (200 µL) consisting of excess $NaNO_3$ (40.0 µmol) and $NaNO_2$ (4.0 µmol) affording $[pCCu_2(\mu\text{-}ONO)](ClO_4)_3$ (**2a**) (black trace) at room temperature.

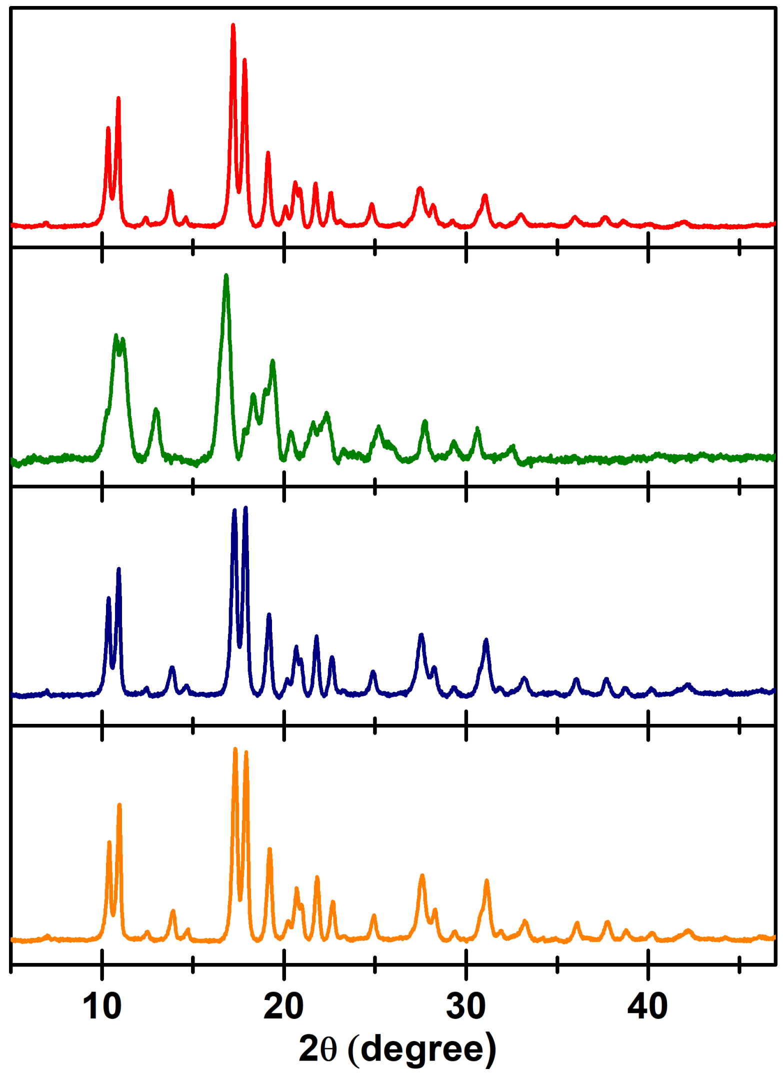

Figure S15. Comparison of PXRD patterns of $[pCCu_2(\mu\text{-}ONO)](ClO_4)_3$ (**2a**) (red trace), $[pCCu_2(\mu\text{-}ONO_2)](ClO_4)_3$ (**2b**) (green trace), $[pCCu_2(\mu\text{-}ONO)](ClO_4)_3$ obtained from a reaction of **2b** + $NaNO_2$ (blue trace), and $[pCCu_2(\mu\text{-}ONO)](ClO_4)_3$ obtained from a reaction of $[pCCu_2]^{4+}$ and a 1:10 mixture of $NaNO_2$ and $NaNO_3$ (orange trace).

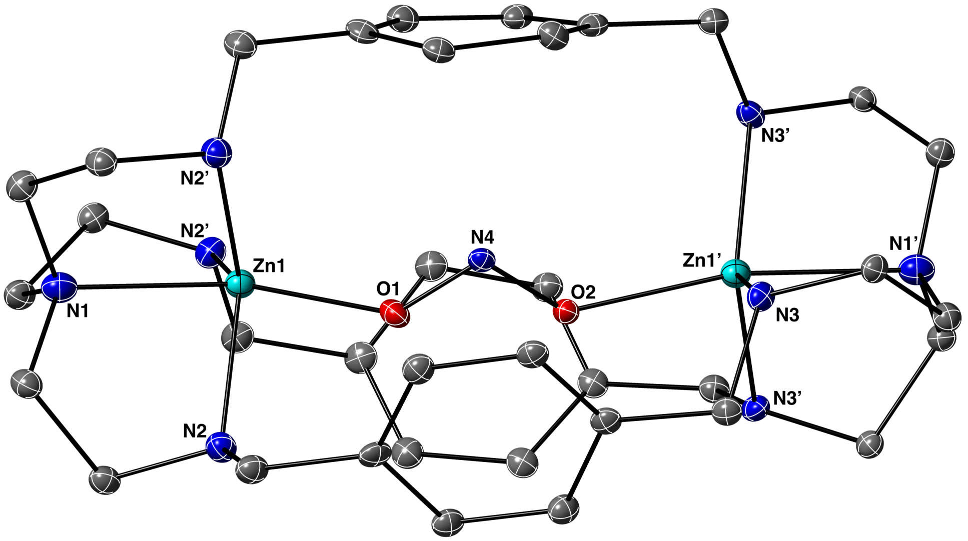

Figure S16. Molecular structure of [pCZn$_2$(μ-ONO)](ClO$_4$)$_3$ (**1a**) (CCDC 1884272). The thermal ellipsoid plots are drawn at 30% probability level. Zn’, N1’, N2’, and N3’ are symmetry generated atoms. Hydrogen atoms and perchlorate anions are omitted for clarity. Selected bond distances (Å) and angles (°) in the primary disorder orientation: Zn1-N1 2.206(14), Zn1-N2 2.13(3), Zn1-O1 1.92(6), N4-O1 1.249(11), N4-O2 1.248(11), Zn1•••Zn’ 6.045, N1-Zn1-O1 168(2), N1-Zn1-N2 82.1(11), N2-Zn1-O1 86(2), O1-N4-O2 114(3).

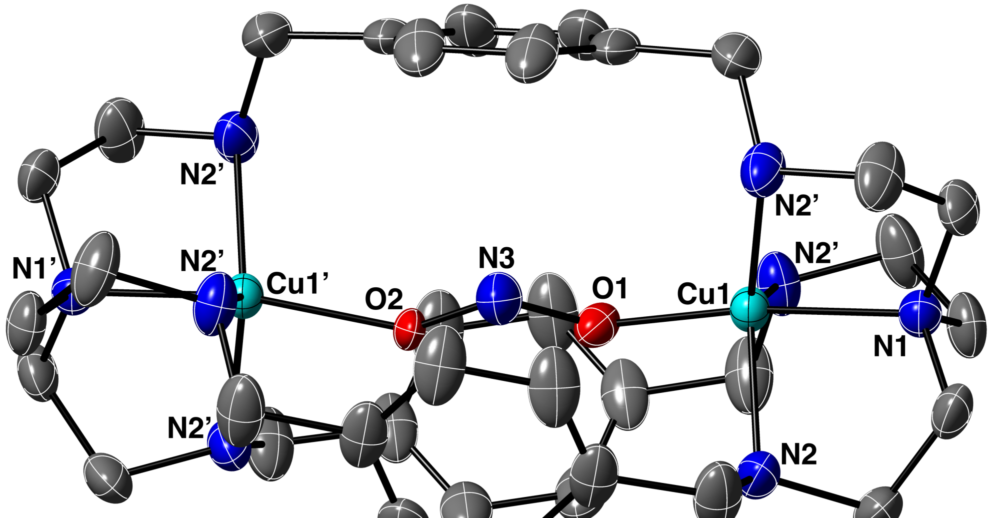

Figure S17. Molecular structure of [pCCu$_2$(μ-ONO)](ClO$_4$)$_3$ (**2a**) (CCDC 1884273). The thermal ellipsoid plots are drawn at 30% probability level. Cu1’, N1’, and N2’ are symmetry generated atoms. Hydrogen atoms and perchlorate anions are omitted for clarity. Selected bond distances (Å) and angles (°) in the primary disorder orientation: Cu1-N1 2.035(6), Cu1-N2 2.129(4), Cu1-O1 1.83(4), N3-O1 1.248(10), N3-O2 1.248(10), Cu1•••Cu’ 6.045, N1-Cu1-O1 172(3), N1-Cu1-N2 84.59(11), N2-Cu1-O1 88(3), O1-N3-O2 128(2).

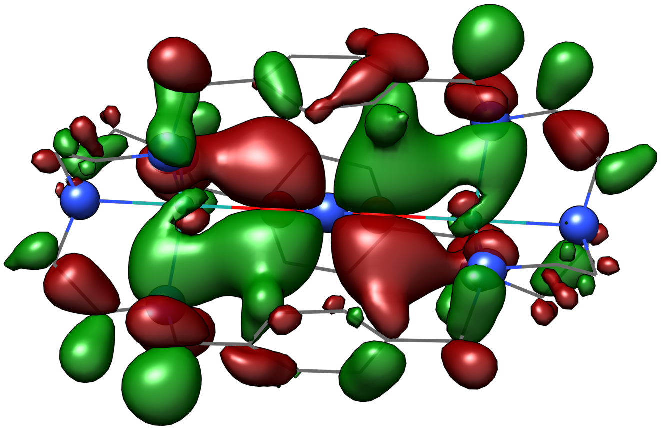

Figure S18. The binding molecular orbital (HOMO-14) of $[pCZn_2(\mu\text{-ONO})]^{3+}$ showing the interactions among $O_{nitrite}$ and the nearest sp^2 carbons of the *p*-xylyl rings as well as $N_{cryptand}$.

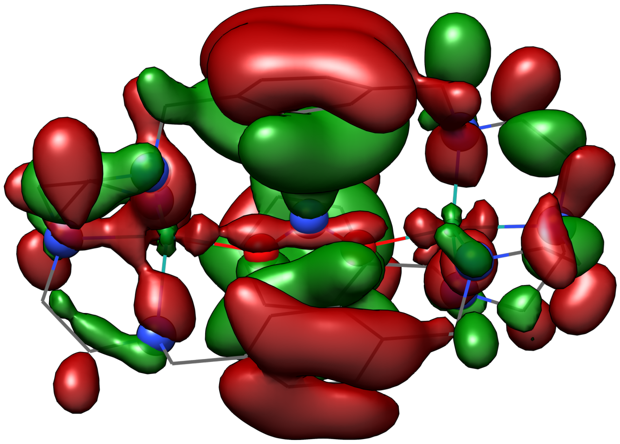

Figure S19. The binding molecular orbital (HOMO-25) of $[pCZn_2(\mu\text{-ONO})]^{3+}$ showing the interaction between $N_{nitrite}$ and the nearest *p*-xylyl ring.

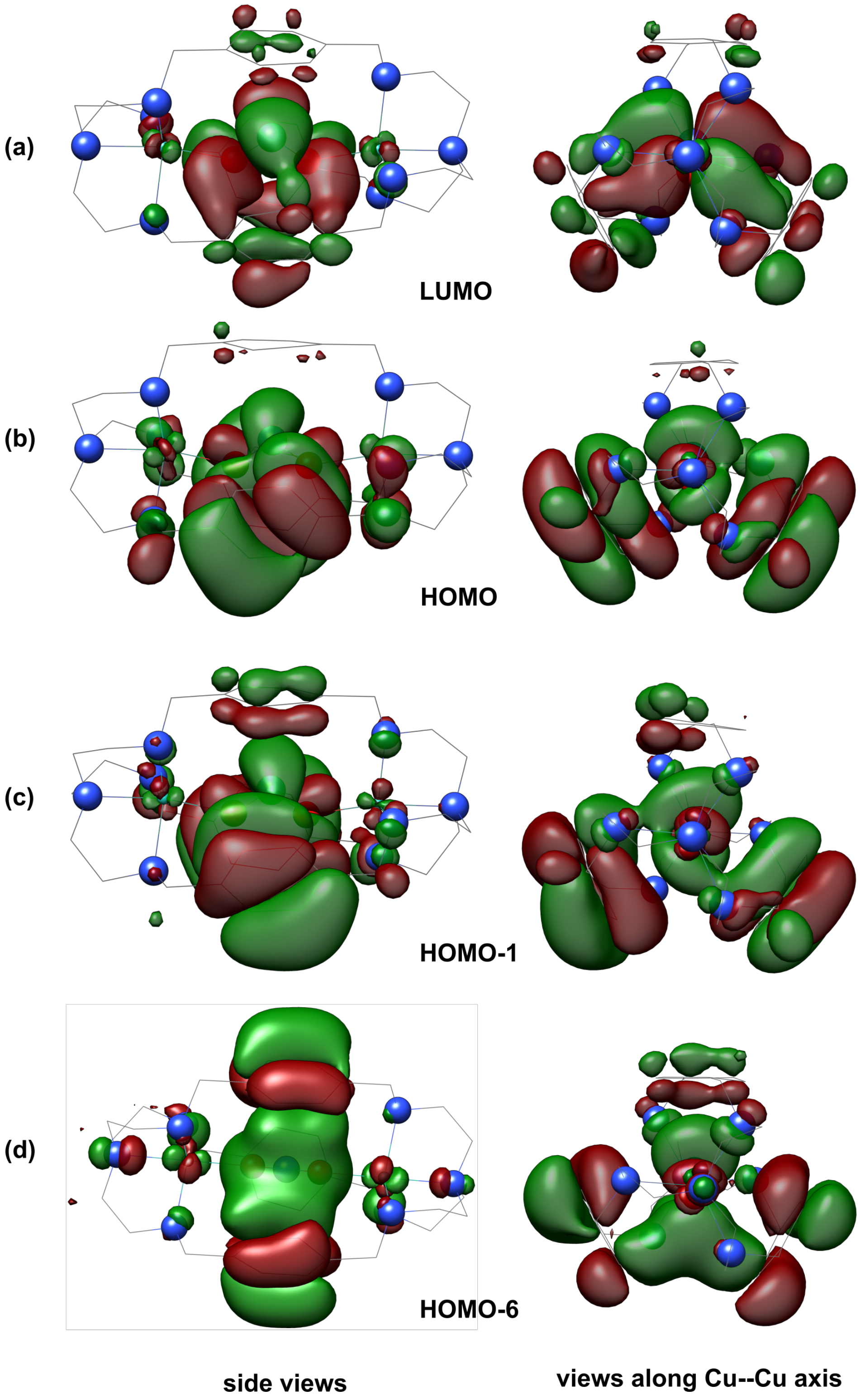

Figure S20. The binding molecular orbitals of $[pCCu_2(\mu\text{-}ONO)]^{3+}$ showing the interactions among $O_{nitrite}$ and the *p*-xylyl spacers.

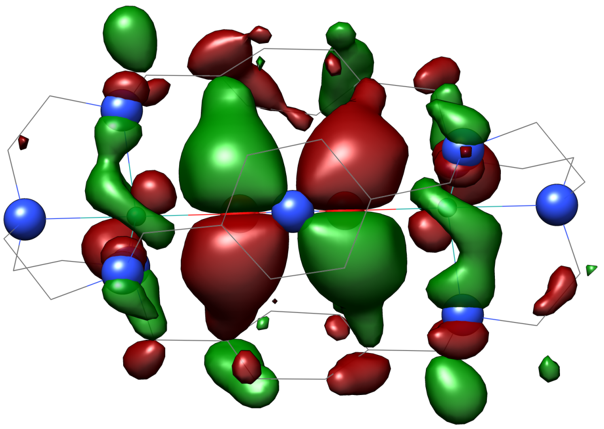

Figure S21. The binding molecular orbital (HOMO-14) of $[pCCu_2(\mu\text{-ONO})]^{3+}$ showing the interactions between $O_{nitrite}$ and the nearest sp^2 carbons of *p*-xylyl rings.

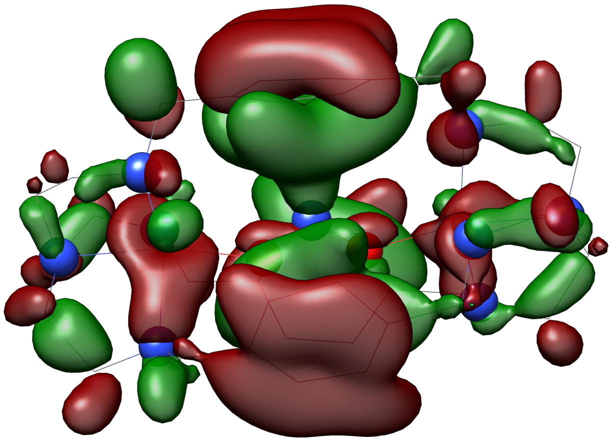

Figure S22. The binding molecular orbital (HOMO-25) of $[pCCu_2(\mu\text{-ONO})]^{3+}$ showing the interactions between $N_{nitrite}$ and the nearest sp^2 carbons of *p*-xylyl ring.

Table S1. Crystallographic data for **1a** and **2a**.

Complex	**1a**	**2a**
CCDC number	1884272	1884273
Empirical formula	$C_{36}H_{54}Cl_3N_9O_{14}Zn_2$	$C_{36}H_{54}Cl_3N_9O_{14}Cu_2$
Formula weight	1073.97	1070.31
Temperature/K	150(2)	296(2)
Crystal system	trigonal	trigonal
Space group	P-31c	P-31c
a/Å	9.758(2)	9.9795(5)
b/Å	9.758(2)	9.9795(5)
c/Å	26.267(9)	25.6934(12)
α/°	90	90
β/°	90	90
γ/°	120	120
Volume/Å^3	2166.2(13)	2216.0(2)
Z	2	2
ρ_{calc}g/cm^3	1.647	1.604
μ/mm^{-1}	1.370	1.216
F(000)	1112.0	1108.0
Crystal size/mm^3	0.200 × 0.150 × 0.150	0.200 × 0.200 × 0.080
Appearance	Colorless	Green
Radiation	MoKα (λ = 0.71073)	MoKα (λ = 0.71073)
2Θ range for data collection/°	1.55 to 50.688	4.714 to 50.73
Index ranges	$-11 \le h \le 11$, $-11 \le k \le 11$, $-31 \le l \le 31$	$-12 \le h \le 11$, $-10 \le k \le 12$, $-30 \le l \le 30$
Reflections collected	21530	26086
Independent reflections	1341 [R_{int} = 0.0922, R_{sigma} = 0.0330]	1365 [R_{int} = 0.0409, R_{sigma} = 0.0159]
Data/restraints/parameters	1341/960/324	1365/154/142
Goodness-of-fit on F^2	1.224	1.158
Final R indexes [I>=2σ(I)]	R_1 = 0.0961, wR_2 = 0.2457	R_1 = 0.0558, wR_2 = 0.1638
Final R indexes [all data]	R_1 = 0.1033, wR_2 = 0.2518	R_1 = 0.0676, wR_2 = 0.1748
Largest diff. peak/hole / e Å^{-3}	1.84/-1.06	0.79/-0.85

Table S2. Comparison of metrical parameters for **1a** and **2a**.

Distance (Å)/ Angle (°)	**1a**		**2a**	
	X-ray	DFT	X-ray	DFT
M-N_{ax}	2.206(14)	2.205	2.035(6)	2.173
M-N_{eq}	2.13(3)	2.107	2.129(4)	2.118
M-O	1.92(6)	2.026	1.83(4)	2.050
N-O	1.249(11)	1.251	1.248(10)	1.255
N-O’	1.248(11)	1.252	1.248(10)	1.258
O-N-O’	114(3)	111.44	128(2)	111.71
$N\cdots C_g$	2.827 3.060 3.392	2.780 3.244 3.251	2.798 3.064 3.561	2.751 3.255 3.272

Table S3. Comparison of Mulliken (MPA) and natural (NPA) population analysis showing electron charges for free nitrite anion and metals, the *p*-xylyl rings, O-N-O moiety in the cations of **1a** and **2a**.

	free NO_2^-		**1a**		**2a**	
	MPA	**NPA**	**MPA**	**NPA**	**MPA**	**NPA**
N	-0.2031	0.1644	0.1260	0.3409	0.1124	0.3447
O	-0.3984 -0.3984	-0.5822 -0.5822	-0.3394 -0.3413	-0.5173 -0.5131	-0.2648 -0.2722	-0.4499 -0.4466
M	-	-	0.8967 0.8526	1.2417 1.2386	0.6164 0.5864	0.9519 0.9397
p-xylyl ring	-	-	0.2432 0.2734 0.2795	0.0752 0.0753 0.0789	0.2267 0.2305 0.2401	0.0780 0.0789 0.0824

12. Cartesian Coordinates of the DFT Optimized Structures (.xyz format)

$[pCZn_2(\mu\text{-}ONO)](ClO_4)_3$ (1a)

C	5.622700	1.338800	-0.421300
C	5.622700	-1.021300	-0.939700
C	5.622500	-0.290300	1.363500
C	4.684200	1.806000	-1.583700
C	4.684000	-2.261600	-0.763200
C	4.683800	0.482700	2.349100
C	2.931600	3.040700	-0.457700
C	2.931800	-1.903400	-2.395800
C	2.931300	-1.109900	2.855000
C	1.435100	3.128600	-0.188200
C	1.435200	-1.713900	-2.606800
C	1.434600	-1.387200	2.796300
C	0.541400	3.065500	-1.341000
C	0.541200	-2.680500	-1.975900
C	0.540900	-0.357400	3.317600
C	-0.864000	3.175200	-1.077100
C	-0.863900	-2.506800	-2.203000
C	-0.864600	-0.640900	3.280700
C	-1.384700	3.083000	0.224800
C	-1.384500	-1.333300	-2.774300
C	-1.384900	-1.722200	2.549800
C	-0.489800	-0.413400	-3.252500
C	-0.490300	-2.596400	1.992400
C	-0.490300	3.037300	1.260600
C	0.904100	3.068400	1.090900
C	0.904500	-0.576100	-3.194200
C	0.904000	-2.464800	2.104400
C	-2.859200	3.078500	0.332200
C	-2.858900	-1.237700	-2.824300
C	-2.859400	-1.813200	2.492000
C	-4.700100	1.881700	1.555900
C	-4.699700	0.420600	-2.399800
C	-4.700000	-2.274700	0.843300
C	-5.602000	1.389300	0.366000
C	-5.601800	-0.363500	-1.378700
C	-5.602000	-0.998100	1.011800
H	2.685600	1.746900	-1.912700
H	2.685500	-2.516600	-0.547800
H	2.685200	0.797100	2.462100
H	-2.741800	1.720300	1.898600
H	-2.741300	0.797900	-2.431200
H	-2.741600	-2.490500	0.532500
H	0.874900	2.956700	-2.223800

$[pCCu_2(\mu\text{-}ONO)](ClO_4)_3$ (2a)

C	5.621100	1.342500	-0.407100
C	5.621300	-1.012300	-0.949500
C	5.621000	-0.304600	1.361000
C	4.682700	1.821300	-1.564800
C	4.682800	-2.254300	-0.785700
C	4.682000	0.458300	2.354300
C	2.929800	3.044400	-0.426400
C	2.930700	-1.879800	-2.414700
C	2.929600	-1.139600	2.844000
C	1.433300	3.129500	-0.156300
C	1.434100	-1.688300	-2.623900
C	1.433200	-1.416400	2.782300
C	0.539700	3.077900	-1.309600
C	0.540100	-2.661300	-2.002800
C	0.539100	-0.392100	3.314000
C	-0.865700	3.184900	-1.044800
C	-0.865100	-2.485500	-2.228300
C	-0.866200	-0.675300	3.274000
C	-1.386500	3.079400	0.256000
C	-1.385700	-1.306100	-2.787600
C	-1.386500	-1.749200	2.532100
C	-0.491100	-0.381400	-3.256400
C	-0.491700	-2.617700	1.966000
C	-0.492100	3.023200	1.291500
C	0.902100	3.056100	1.122100
C	0.903200	-0.544500	-3.199700
C	0.902500	-2.487000	2.079400
C	-2.860900	3.073700	0.363400
C	-2.860100	-1.210200	-2.836800
C	-2.860900	-1.839700	2.473400
C	-4.701900	1.864300	1.574700
C	-4.701100	0.443500	-2.395700
C	-4.701400	-2.284600	0.819900
C	-5.603500	1.384000	0.379800
C	-5.603100	-0.351100	-1.382600
C	-5.603400	-1.009800	1.001300
H	2.684100	1.765400	-1.894500
H	2.684300	-2.511800	-0.573100
H	2.683500	0.771300	2.470400
H	-2.743500	1.699600	1.915900
H	-2.742700	0.821300	-2.423000
H	-2.742900	-2.497100	0.507000
H	0.873300	2.978100	-2.193400

H	0.874600	-3.390700	-1.440300
H	0.874200	0.461600	3.664900
H	-1.460200	3.314400	-1.803500
H	-1.460200	-3.205400	-1.960500
H	-1.460800	-0.081500	3.764300
H	-0.831700	0.380600	-3.646400
H	-0.832200	-3.334600	1.501700
H	-0.832300	2.981500	2.145100
H	1.479200	0.088900	-3.554800
H	1.478700	-3.109600	1.708900
H	1.478700	3.048200	1.847000
H	6.561300	1.301400	-0.734000
H	6.561300	-1.273500	-0.750700
H	6.561000	-0.000600	1.487500
H	5.569700	1.973500	0.336700
H	5.569800	-0.682200	-1.868400
H	5.569500	-1.264000	1.534000
H	4.941700	2.715300	-1.878600
H	4.941700	-2.971500	-1.403100
H	4.941200	0.283500	3.284000
H	4.774100	1.192400	-2.355300
H	4.773700	-2.623000	0.154000
H	4.773700	1.457900	2.203500
H	3.207900	3.797800	-1.032500
H	3.207900	-2.779900	-2.764100
H	3.207300	-0.990700	3.798200
H	3.424800	3.109600	0.398000
H	3.425100	-1.197000	-2.883200
H	3.424700	-1.885300	2.487000
H	-3.261400	3.098300	-0.572200
H	-3.261200	-2.030700	-2.389400
H	-3.261700	-1.040000	2.961200
H	-3.161500	-1.214000	-3.766700
H	-3.162200	-2.641200	2.942600
H	-3.161900	3.882800	0.823800
H	-4.926200	0.165200	-3.329100
H	-4.926700	-2.951600	1.529100
H	-4.926600	2.814200	1.799300
H	-4.830900	1.306200	2.350700
H	-4.830400	1.396700	-2.298900
H	-4.830800	-2.675100	-0.052500
H	-6.554500	1.446800	0.629100
H	-6.554400	-0.164300	-1.560200
H	-6.554600	-1.254700	0.929800
H	-5.464200	1.978600	-0.417400
H	-5.464000	-1.336700	-1.497300

H	0.873600	-3.376900	-1.474400
H	0.872400	0.423400	3.669600
H	-1.461700	3.331300	-1.769800
H	-1.461300	-3.186500	-1.992900
H	-1.462500	-0.120800	3.763300
H	-0.832900	0.416500	-3.642300
H	-0.833600	-3.350800	1.467800
H	-0.834300	2.958300	2.175300
H	1.478100	0.124000	-3.553500
H	1.477300	-3.127700	1.677500
H	1.476800	3.028300	1.878000
H	6.559800	1.308200	-0.720100
H	6.559900	-1.266300	-0.763000
H	6.559400	-0.016100	1.488000
H	5.568000	1.969400	0.357200
H	5.568500	-0.663700	-1.874600
H	5.568000	-1.280100	1.521600
H	4.940100	2.733600	-1.850500
H	4.940500	-2.957700	-1.432800
H	4.939400	0.249600	3.287200
H	4.772700	1.215600	-2.342600
H	4.772400	-2.625000	0.127900
H	4.771800	1.434900	2.218600
H	3.206100	3.807400	-0.993500
H	3.206900	-2.752400	-2.791800
H	3.205700	-1.030000	3.788300
H	3.423100	3.104800	0.429900
H	3.423900	-1.168400	-2.894800
H	3.423200	-1.911200	2.468100
H	-3.263200	3.102600	-0.540700
H	-3.262400	-2.007700	-2.410000
H	-3.263400	-1.071300	2.950300
H	-3.162600	-1.177100	-3.778900
H	-3.163700	-2.672100	2.915500
H	-3.163900	3.872900	0.863100
H	-4.927500	0.197500	-3.327500
H	-4.928000	-2.968500	1.498800
H	-4.928500	2.794300	1.827500
H	-4.832700	1.280700	2.363600
H	-4.831800	1.418500	-2.284800
H	-4.832000	-2.676000	-0.079900
H	-6.556200	1.438700	0.643500
H	-6.555700	-0.150100	-1.562100
H	-6.556000	-1.265800	0.916700
H	-5.465800	1.981300	-0.397600
H	-5.465300	-1.323000	-1.511100

H	-5.464500	-0.614300	1.913800
N	5.177100	0.009100	0.000700
N	-5.280300	0.009300	-0.000100
N	3.264700	1.810800	-1.099900
N	3.264700	-1.844700	-1.009500
N	3.264500	0.061300	2.111100
N	-3.318000	1.797300	1.084900
N	-3.317800	0.054900	-2.091000
N	-3.318100	-1.824400	1.005900
N	-0.023600	0.313800	-0.004500
O	1.003700	-0.402600	-0.004400
O	-1.064700	-0.379700	-0.000100
Zn	2.985200	0.018500	-0.001600
Zn	-3.061500	0.017300	0.001100

H	-5.466100	-0.635200	1.907200
N	5.175600	0.008500	0.001300
N	-5.281800	0.007800	-0.000400
N	3.263100	1.821100	-1.081100
N	3.263400	-1.835100	-1.027700
N	3.262800	0.039100	2.111900
N	-3.319800	1.784800	1.103000
N	-3.319100	0.074900	-2.090500
N	-3.319500	-1.835900	0.987200
N	-0.017200	0.341800	-0.007100
O	1.019200	-0.371800	-0.004200
O	-1.060900	-0.355200	-0.001900
Cu	3.020900	0.012600	-0.003600
Cu	-3.089900	0.014100	0.001900

13. References

(S1) P. S. Lakshminarayanan, I. Ravikumar, E. Suresh and P. Ghosh, *Cryst. Growth Des.*, **2008**, *8*, 2842–2852.

(S2) L. Z. Yang, Y. Li, X. M. Zhuang, L. Jiang, J. M. Chen, R. L. Luck and T. B. Lu, *Chem. Eur. J.*, **2009**, *15*, 12399–12407.

(S3) A. D. Bond, S. Derossi, F. Jensen, F. B. Larsen, C. J. McKenzie and J. Nelson, *Inorg. Chem.*, **2005**, *44*, 5987–5989.

(S4) (a) SHELXTL-PC, Vers. 5.10; 1998, Bruker-Analytical X-ray Services, Madison, WI. (b) G. M. Sheldrick, SHELX-97, Universität Göttingen, Göttingen, Germany.

(S5) SADABS; G. M. Sheldrick, 1996, based on the method described in R. H. Blessing, *Acta Crystallogr. Sect. A*, **1995**, *51*, 33-38.

(S6) Gaussian 09, Revision A.02, M. J. Frisch, G. W. Trucks, H. B. Schlegel, G. E. Scuseria, M. A. Robb, J. R. Cheeseman, G. Scalmani, V. Barone, B. Mennucci, G. A. Petersson, H. Nakatsuji, M. Caricato, X. Li, H. P. Hratchian, A. F. Izmaylov, J. Bloino, G. Zheng, J. L. Sonnenberg, M. Hada, M. Ehara, K. Toyota, R. Fukuda, J. Hasegawa, M. Ishida, T. Nakajima, Y. Honda, O. Kitao, H. Nakai, T. Vreven, J. A. Montgomery, Jr., J. E. Peralta, F. Ogliaro, M. Bearpark, J. J. Heyd, E. Brothers, K. N. Kudin, V. N. Staroverov, R. Kobayashi, J. Normand, K. Raghavachari, A. Rendell, J. C. Burant, S. S. Iyengar, J. Tomasi, M. Cossi, N. Rega, J. M. Millam, M. Klene, J. E. Knox, J. B. Cross, V. Bakken, C. Adamo, J. Jaramillo, R. Gomperts, R. E. Stratmann, O. Yazyev, A. J. Austin, R. Cammi, C. Pomelli, J. W. Ochterski, R. L. Martin, K. Morokuma, V. G. Zakrzewski, G. A. Voth, P. Salvador, J. J. Dannenberg, S. Dapprich, A. D. Daniels, O. Farkas, J. B. Foresman, J. V. Ortiz, J. Cioslowski, and D. J. Fox, Gaussian, Inc., Wallingford CT, 2009.

(S7) (a) J. P. Perdew, *Phys. Rev. B* **1986**, *34*, 7406-7406. (b) C. T. Lee, W. T. Yang, R. G. Parr, *Phys. Rev. B* **1988**, *37*, 785-789. (c) J. P. Perdew, *Phys. Rev. B* **1989**, *33*, 8822-8824.

(S7) (a) A. Schäfer, H. Horn, R. Ahlrichs, *J. Chem. Phys.,* **1992**, *97*, 2571-2577. (b) A. Schäfer, H. Horn, R. Ahlrichs, *J. Chem. Phys.* **1994**, *100*, 5829-5835. (c) F. Weigend, R. Ahlrichs, *Phys. Chem. Chem. Phys.,* **2005**, *7*, 3297-3305.

(S8) (a) A. E. Reed and F. Weinhold, *J. Chem. Phys.* **1983**, *78*, 4066-4073. (b) A. E. Reed, R. B. Weinstock, and F. Weinhold, *J. Chem. Phys.* **1985**, *83*, 735-746.

(S9) GaussView, Version 5, R. Dennington, T. A. Keith, and J. M. Millam, Semichem Inc., Shawnee Mission, KS, 2009.

(S10) (a) http://www.rbvi.ucsf.edu/chimera/1.9/docs/credits.html; (b) UCSF Chimera; E. F. Pettersen, T. D. Goddard, C. C. Huang, G. S. Couch, D. M. Greenblatt, E. C. Meng, T. E. Ferrin, *J. Comput. Chem.* **2004**, *25*, 1605-1612.

(S11) CCDC Mercury Version 3.8; C. F. Macrae, P. R. Edgington, P. McCabe, E. Pidcock, G. P. Shields, R. Taylor, M. Towler and J. van de Streek, *J. Appl. Cryst.* **2006**, *39*, 453-457.